Temporal dispersion of a spectrometer[a)]

A. Visco,[1] R. P. Drake,[1] D. H. Froula,[2] S. H. Glenzer,[2] and B. B. Pollock[2]
[1]*University of Michigan, 2455 Hayward, Ann Arbor, Michigan 48109, USA*
[2]*Lawrence Livermore National Laboratory, L-399, P.O. Box 808, Livermore, California 94551, USA*

(Presented 15 May 2008; received 12 May 2008; accepted 25 July 2008; published online 31 October 2008)

The temporal dispersion of an optical spectrometer has been characterized for a variety of conditions related to optical diagnostics to be fielded at the National Ignition Facility (e.g., full-aperture backscatter station, Thomson scattering). Significant time smear is introduced into these systems by the path length difference through the spectrometer. The temporal resolution is shown to depend only on the order of the grating, wavelength, and the number of grooves illuminated. To enhance the temporal resolution, the spectral gratings can be masked limiting the number of grooves illuminated. Experiments have been conducted to verify these calculations. The size and shape of masks are investigated and correlated with the exact shape of the temporal instrument function, which is required when interpreting temporally resolved data. The experiments used a 300 fs laser pulse and a picosecond optical streak camera to determine the temporal dispersion. This was done for multiple spectral orders, gratings, and optical masks. © *2008 American Institute of Physics.*
[DOI: 10.1063/1.2972022]

I. INTRODUCTION

Optical spectrometers are instruments employed by several diagnostics systems at many high energy density facilities, including the full-aperture backscattering station (FABS) at the National Ignition Facility.[1] FABS is designed to measure the backscattered light from stimulated Raman scattering (SRS) and stimulated Brillouin scattering (SBS) instabilities in plasmas. For SBS and SRS the wavelength is sensitive to electron temperature and the electron density, respectively.[2] Furthermore, experiments at the Nova Laser facility have demonstrated the accuracy of Thomson scattering in the measurement of densities, electron temperatures, and average ionization levels.[3] Additional experiments have used the Thomson scattering technique to measure incoherent and collective features of laboratory plasmas.[4,5] Since plasmas produced by intense laser light are often short lived, with parameters changing on the time scale of tens to hundreds of picoseconds, temporal resolution of spectral features are important to investigating these plasmas. One limitation on the temporal resolution is the time smear introduced by the spectrometer. The optical path length through the spectrometer varies for rays reflected from different parts of the grating, causing a delay for different parts of the pulse. The difference in path length is calculated and shown to only depend on order, wavelength, and number of grooves illuminated. We report an experiment conducted to test these calculations. The temporal dispersion was measured for many gratings and spectral orders. Masks were used to limit the number of grooves illuminated as well as to study the relationship between the area of the grating illuminated and the temporal instrument function.

[a)]Contributed paper, published as part of the Proceedings of the 17th Topical Conference on High-Temperature Plasma Diagnostics, Albuquerque, New Mexico, May 2008.

II. THEORY

The temporal broadening introduced by a spectrometer shown in Fig. 1 is a result of the path length difference light travels through the spectrometer. In a standard spectrometer with reflective optics, the only path difference is introduced by the effects of diffraction at the grating. The path difference of radiation reflected from adjacent groves, Δl, is given by

$$\Delta l = d(\sin\alpha + \sin\beta), \tag{1}$$

corresponding to

$$\Delta l_{\mathrm{tot}} = nd(\sin\alpha + \sin\beta), \quad \text{or}$$

$$\Delta l_{\mathrm{tot}} = nm\lambda_0, \tag{2}$$

where m is the order, n is the total number of grooves illuminated, and λ_0 is the wavelength of the laser. Photons arriving at the detector from opposite ends of the grating are thus offset temporally by

$$\delta t_g = \frac{nm\lambda_0}{c}. \tag{3}$$

As seen from Eqs. (2) and (3), there is no broadening for the zero order case for which $\alpha=-\beta$. This is sensible as the zeroth-order case corresponds to a purely reflective imaging system, through which all optical paths are equal.

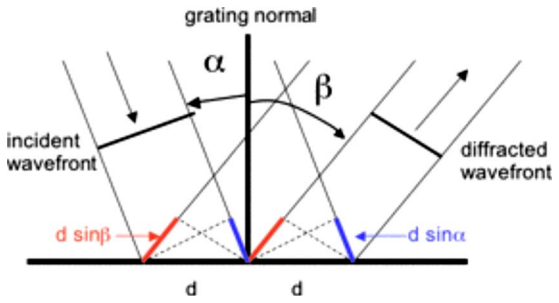

FIG. 1. (Color online) Grating geometry is shown. Path differences along the length of the grating are one cause of the temporal smearing. The angle labeled as β in the figure is actually negative β, given the measurement convention described in the text.

III. EXPERIMENT

To measure the time smear introduced by the grating, a 300 fs laser pulse was propagated through a Czerny–Turner spectrometer and imaged by a streak camera (Hamamatsu C7700-S20). A 1 m diffraction grating spectrometer (Acton, AM510) was employed for the experiment. The theory of diffraction grating spectrometry is well established and can be found elsewhere.[5–7] The laser pulse duration is much smaller than the time resolution of the spectrometer, thus any variation or structure in the pulse is unresolvable and any measured temporal profile can be attributed to optical path differences across the grating. To measure the temporal dispersion, a 1ω (1053 nm) laser pulse is frequency doubled and sent through the spectrometer. The resulting 2ω light is focused in the plane of the entrance slit using an $f/5$ lens that, when passing through the entrance slit, slightly overfills the $f/\#$ of the spectrometer ($f/7$), ensuring that the grating is fully illuminated. The streak camera slit is aligned to the exit plane of the spectrometer.

The streak camera was operated at various sweep speeds from 0.5 to 5 ns, depending on available laser signal. The temporal resolution of the streak camera is ~1% of sweep time, making any broadening introduced by the camera negligible compared to the dispersion introduced by the grating.

The temporal smearing was measured for 300, 1200, 1800, and 2400 lines/mm gratings and for five spectral orders using the 300 lines/mm grating. To test the dependence of the broadening on the number of grooves illuminated, measurements were made using a variety of optical masks. The masks were placed in front of the first spherical mirror

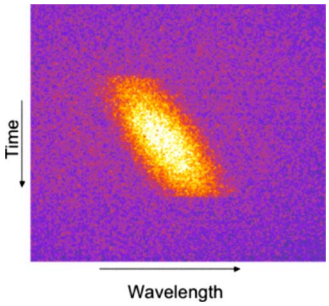

FIG. 2. (Color online) Raw data obtained from streak camera for a 1800 lines/mm grating and a sweep time of 1 ns.

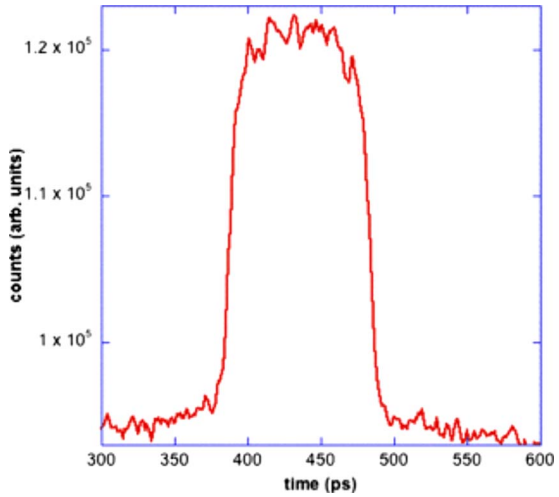

FIG. 3. (Color online) Temporal profile of a measured pulse. The sharp rise and fall of the intensity define the temporal width of the pulse.

to limit the area of the grating that is illuminated by the laser. Different mask geometries were used and correlated with the temporal instrument function.

IV. RESULTS

Figure 2 is a typical image recorded by the streak camera, in this case using an 1800 lines/mm grating and a 1 ns sweep. The 300 fs pulse has been stretched out by the spectrometer to ~300 ps. Light imaged at different times is reflected from different parts of the grating. Another feature seen in the image is the temporal separation of wavelengths or "chirp" introduced by the finite bandwidth of the laser and the slight variations of incident angle across the grating. A chirp is a signal in which the frequency changes in time. One observes the chirp in the spectrum detected by the streak camera; longer wavelengths arrive later in time. It is worthwhile to discuss the origin of this effect in the present data and then its relevance to the more complex spectra of interest

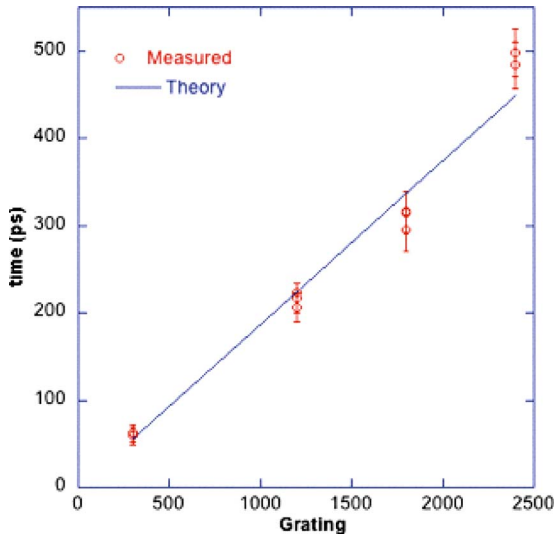

FIG. 4. (Color online) Dependence of temporal dispersion on the number of grooves illuminated. Different gratings are employed to vary the number of grooves illuminated.

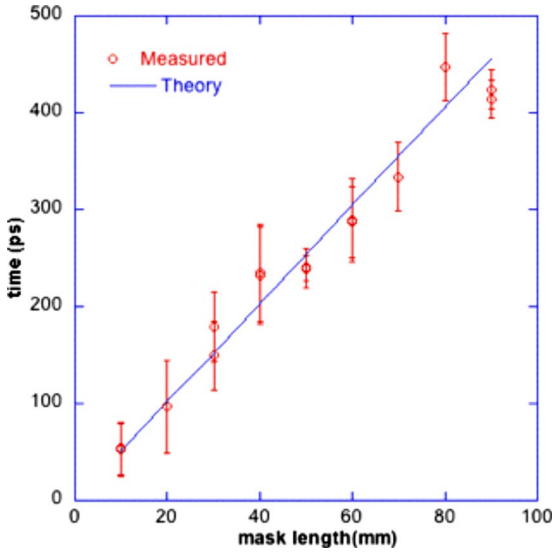

FIG. 5. (Color online) Dependence of temporal dispersion on the number of grooves illuminated. Masks are used to restrict how much of the grating is illuminated.

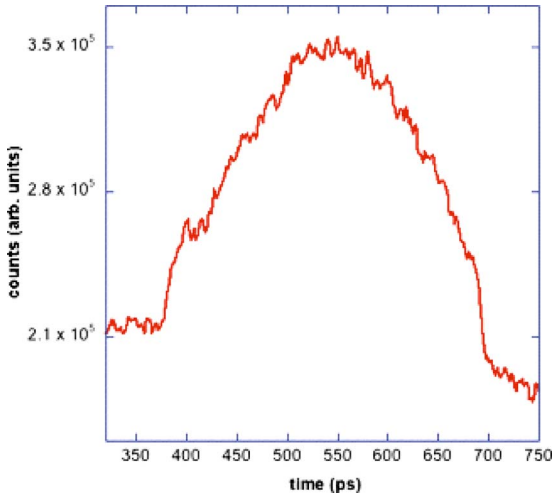

FIG. 7. (Color online) Effect of a spatially nonuniform beam on the temporal instrument function. Variations in intensity across the grating result in temporal variation in the image.

for applications. The chirp arises because short pulses inherently have large bandwidth. Specifically, any feature in the signal having a duration $\Delta\tau$ will necessarily have a frequency spread of at least $\Delta f=(2\pi\Delta\tau)^{-1}$ cycles/s. To understand the chirp at the exit plane of the spectrometer, it is important to realize that both the time the light arrives at the spectrometer and its wavelength are directly related to the position on the grating from which it was reflected. Light coming from the end of the grating closer to the camera arrives earlier than light from the grating's opposite end. Furthermore, light incident on different parts of the grating will make different angles with respect to the grating normal, corresponding to different wavelengths that satisfy the grating equation. The signal observed at any given wavelength on the exit plane is produced by only a limited number of grooves on the grating, and correspondingly experiences less smearing in time than the total signal does. If one can clearly see such a chirp in data, one can infer something about the duration of the event that produced the signal. In contrast, in an application producing a complex spectrum (or with large spectral bandwidth compared to Δf), one may well be unable to observe the chirp. In this case the time resolution of the measurement corresponds to the total duration of the signals observed in the present measurements and described by the theoretical relations above.

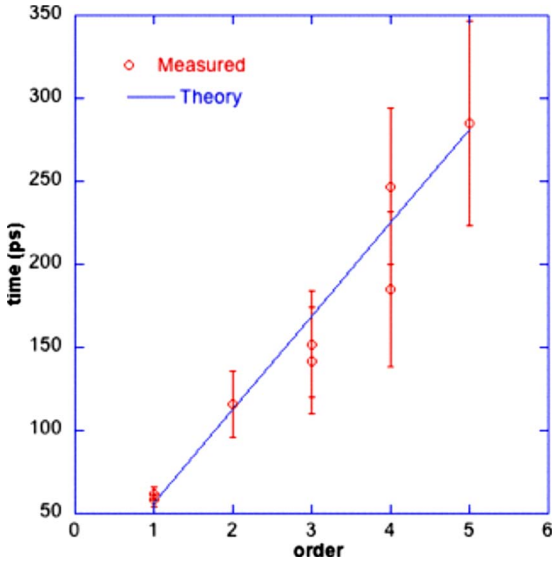

FIG. 6. (Color online) Dependence of temporal dispersion on spectral order.

Figure 3 shows a temporal profile of a measurement made in first order ($m=1$) with $n\sim 28\,700$ grooves illuminated. A polynomial function is fit to the background noise and two lines are fit to the sharp rise and fall of the signal. The intersection of the two edge lines with the polynomial define the beginning and end of the pulse, which defines the temporal dispersion (δt_g). The error bars in later figures reflect our assessment of the accuracy with which δt_g can be determined from the data.

Figure 4 shows a linear relation between the number of grooves illuminated and the temporal broadening. Different gratings were used to change the number of grooves illuminated. To vary the length of the grooves in the grating being illuminated, spectral masks were employed. Using square masks of varying sizes, it can be seen that the temporal broadening of the pulse depends on the length of the grating orthogonal to the grooves. Masking of the height of the grating only serves to reduce the transmission of the system. The mask was put in front of the mirror, therefore the projection of the mask onto the grating was used to determine the number of grooves illuminated. In Fig. 5, the broadening is seen to be linear with respect to the number of grooves illuminated, as predicted by the theory.

In a similar fashion, the dependence of the dispersion on spectral order was measured using the 300 lines/mm grating for several spectral orders ($m=1,2,3,4,5$). For higher spectral orders, the signal intensity was only slightly above the background, creating greater errors in the method for measuring the broadening. Figure 6 shows the results of the measurement.

Figure 7 shows a measurement made when the grating

was not uniformly filled; namely, the intensity peaked at the center falling off significantly at the edges. Since the laser spot is imaged onto the grating, any variation in intensity along the length of the grating (orthogonal to grooves) will be detected as an intensity variation in time in the streak camera image. Variations in the beam profile can be clipped out by employing an optical mask on the spherical mirror.

V. CONCLUSIONS

The time smear introduced from path length through the detector has been analyzed and found to depend only on the order of the grating, wavelength, and the number of grooves illuminated, in accordance with the theory developed. Furthermore, the shape of the instrument function is related to the intensity distribution on the grating and the effects introduced by optical masks were discussed and correlated with the temporal instrument function.

ACKNOWLEDGMENTS

This work was performed under the auspices of the U.S. Department of Energy by the Lawrence Livermore National Laboratory under Contract No. DE-AC52-07NA27344.

[1] D. H. Froula, D. Bower, M. Chrisp, S. Grace, J. H. Kamperschroer, T. M. Kelleher, R. K. Kirkwood, B. MacGowan, T. McCarville, N. Sewall, F. Y. Shimamoto, S. J. Shiromizu, B. Young, and S. H. Glenzer, Rev. Sci. Instrum. **75**, 4168 (2004).
[2] W. L. Kruer, *The Physics of Laser Plasma Interactions* (Addison-Wesley, Reading, MA, 1988).
[3] E. M. Campbell, Laser Part. Beams **9**, 209 (1991).
[4] S. H. Glenzer, C. A. Back, K. G. Estabrook, R. Wallace, K. Baker, B. J. MacGowan, B. A. Hammel, R. E. Cid, and J. S. De Groot, Phys. Rev. Lett. **77**, 1496 (1996).
[5] S. H. Glenzer, G. Gregori, F. J. Rogers, D. H. Froula, S. W. Pollaine, R. S. Wallace, and O. L. Landen, Phys. Plasmas **10**, 2433 (2003).
[6] J. Sheffield, *Plasma Scattering of Electromagnetic Radiation* (Academic, New York, 1975).
[7] M. Born and E. Wolf, *Principles of Optics*, 7th ed. (Cambridge University Press, Cambridge, UK, 1999).